ANNALS of Clinical and Translational Neurology
Open Access
ANA American Neurological Association since 1875

RESEARCH ARTICLE

Ixabepilone-induced mitochondria and sensory axon loss in breast cancer patients

Gigi J. Ebenezer[1,a], Karen Carlson[2,a], Diana Donovan[2], Marta Cobham[2], Ellen Chuang[2], Anne Moore[2], Tessa Cigler[2], Maureen Ward[2], Maureen E. Lane[2], Anita Ramnarain[2], Linda T. Vahdat[2,b] & Michael Polydefkis[1,b]

[1]Neurology, Johns Hopkins University, Baltimore, Maryland
[2]Breast Cancer Research Program, Weill Cornell Medical College, New York City, New York

Correspondence
Michael Polydefkis, Johns Hopkins Neurology, 855 N. Wolfe Street, Rangos Building 435, Baltimore, MD 21205. Tel: 410-502-2909 (office); 410-955-3254 (lab); Fax: 410-502-5560; E-mail: mpolyde@jhmi.edu

Funding Information
Bristol Myers Squibb Oncology (BMSO) and the Anne Moore Breast Cancer Research Fund provided partial funding for this study. BMSO also provided study drug.

Received: 27 May 2014; Revised: 25 June 2014; Accepted: 15 July 2014

***Annals of Clinical and Translational Neurology* 2014; 1(9): 639–649**

doi: 10.1002/acn3.90

[a,b]These authors contributed equally.

Abstract

Background: We sought to define the clinical and ultrastructure effects of ixabepilone (Ix), a microtubule-stabilizing chemotherapy agent on cutaneous sensory nerves and to investigate a potential mitochondrial toxicity mechanism. **Methods**: Ten breast cancer patients receiving Ix underwent total neuropathy score clinical (TNSc) assessment, distal leg skin biopsies at cycle (Cy) 3 (80–90 mg/m^2), Cy5 (160–190 mg/m^2), and Cy7 (>200 mg/m^2) and were compared to 5 controls. Skin blocks were processed for EM and ultrastructural morphometry of Remak axons done. **Results**: At baseline, Ix-treated subjects had higher TNSc values (4.5 ± 0.8 vs. 0.0 ± 0.0), greater percentage of empty (denervated) Schwann cells (29% vs. 12%), altered axonal diameter (422.9 ± 17 vs. 354.9 ± 14.8 nm, $P = 0.01$), and axon profiles without mitochondria tended to increase compared to control subjects (71% vs. 70%). With increasing cumulative Ix exposure, an increase in TNSc values (Cy3: 5.4 ± 1.2, Cy7: 10 ± 4, $P < 0.001$), empty Schwann cells (39% by Cy7), and dilated axons (in nm, Cy3: 506.3 ± 22.1, Cy5: 534.8 ± 33, Cy7: 527.8 ± 24.4; $P < 0.001$) was observed. In addition, axon profiles without mitochondria (Cy3:74%, Cy7:78%) and mitochondria with abnormal morphology (grade 3 or 4) increased from 24% to 79%. Schwann cells with atypical mitochondria and perineuronal macrophage infiltration in dermis were noted. **Interpretation**: This study provides functional and structural evidence that Ix exposure induces a dose-dependent toxicity on small sensory fibers with an increase in TNSc scores and progressive axonal loss. Mitochondria appear to bear the cumulative toxic effect and chemotherapy-induced toxicity can be monitored through serial skin biopsy-based analysis.

Introduction

Increases in breast cancer survival can be attributed to many factors including development of improved chemotherapy agents.[1,2] Microtubule-stabilizing agents (MTSA) such as taxanes are the backbone of nearly all early and later line therapy.[3,4] Newer chemotherapy agents such as the epothilones are a novel class of MTSA with demonstrated antitumor activity in a broad spectrum of indications including in taxane-resistant tumors.[5–7] Ixabepilone, an epothilone analogue received FDA approval in 2007 for metastatic and locally advanced breast cancer. As with all MTSA-based regimens,[8] ixabepilone is associated with chemotherapy-induced peripheral neuropathy (CIPN) that decreases quality of life and can alter subsequent ability to receive additional MTSA-based chemotherapy regimens with unknown effects on survival.[9] Predominant involvement of small distal sensory nerve fibers has been observed across clinical studies of ixabepilone (phases I–III) in patients with early and metastatic disease.[5,7,10–13] A meta-analysis of six different clinical studies based on NCI grading reveals that the incidence of grade 3 or 4 neuropathy increases with additional cycles of treatment indicating the cumulative

nature of the toxicity.[13] While animal model data have shown that epothilones induce a dose-limiting neurotoxicity and recovery after withdrawal of treatment,[14] there is no longitudinal pathological human data to confirm this finding.

Both taxanes and epothilones interfere with polymerization of tubulin dimers and stabilize preformed microtubules against conditions favoring depolymerization.[15,16] Epothilones bind to β-tubulin at a molecular epitope distinct from the one bound by taxanes, suggesting different neurotoxicity profiles.[17,18] Skin biopsies from the distal leg have been used for diagnostic purposes in patients with clinically doubtful small fiber neuropathy to evaluate the loss of the most distal sensory nerve endings, typical of length-dependent axonal neuropathy.[19,20] Preclinical studies have suggested that mitochondrial toxicity is a shared mechanism across numerous chemotherapy agents.[21] The goal of this study was to rigorously assess changes in peripheral nerve (PN) function and structure in patients receiving ixabepilone for breast cancer as part of a phase II clinical trial.

Materials and Methods

Study subjects

Ten female patients receiving ixabepilone chemotherapy for three or more cycles (Cy) as part of a phase II clinical trial for advanced breast cancer were enrolled after Institutional Review Board approval (IRB# 0707009284, NCT00627978). Written informed consent was obtained prior to undergoing any study-specific procedures in accordance with the Declaration of Helsinki.

Nine subjects were white (7), Hispanic (1), or South Asian (1) and one subject was African American. No subject had diabetes while two had controlled hypertension and five had a history of remote tobacco use. Ixabepilone (Ix) was provided by Bristol Myers Squibb Oncology. Four subjects received weekly Ix infusions (16 mg/m^2 IV over 1 h, 3 weeks on, 1 week off), whereas six subjects received q3-week infusions (40 mg/m^2, IV over 3 h, once every 3 weeks). Four of these six subjects subsequently converted to the weekly regimen because of toxicity (two gastrointestinal and two peripheral neuropathy). All subjects underwent clinical evaluation with calculation of a total neuropathy score clinical (TNSc)[22] at baseline and every two cycles (third, fifth, and seventh Cy) while on study. The ixabepilone dosing schedule and clinical/skin biopsy evaluations are given in Table 1.

All patients had skin biopsies at study entry and eight of 10 had a second biopsy. Seven are included in this analysis.

Skin biopsies and electron microscopic studies

Skin punches (3 mm) were performed 10 cm above the lateral malleolus on seven patients and five controls. The biopsies were processed for 48 h in 4% paraformaldehyde −3% glutaraldehyde fixative and then transferred to 0.1 mol/L Sorensen's phosphate buffer. Sections were post-fixed with osmium and embedded in plastic. The samples were embedded vertically so that the sections went through epidermis and dermis to a depth of 1500 μm from epidermal dermal junction and thin 60- to 70-nm sections were mounted on Formvar-coated (Sigma-Aldrich, St. Louis, MO, USA) 50- or 100-mesh grids and stained with uranyl acetate (2.5% in 50% ethanol) and lead citrate (3%). Under a digital Zeiss Libra 120 transmission electron microscope (Carl Zeiss Microscopy, New York, USA) the outline of the skin sections was traced and by a stepwise

Table 1. Dosage schedule of study patients.

No	Age (years)	Initial Ix study arm	Initial Ix dose (mg/m^2)	Total cumulative dose at Cy3 (mg/m^2)	Total cumulative dose at Cy5 (mg/m^2)	Total cumulative dose at Cy7 (mg/m^2)	Total dose received (mg/m^2)	Baseline TNSc
1[1]	54	q1 wk	16	96	192	288	144	2
2[2]	66	q1 wk	16	80	160	232	528	1
3[1,2]	55	q3 wks	40	80	120		204	7
4	39	q3 wks	40	96	144		120	2
5[2]	58	q1 wk	16	80	160	242	400	5
6[1]	70	q3 wks	40	80	160	232	268	5
7[2]	52	q1 wk	16	96	192	288	464	7
8[1,2]	64	q3 wks	40	80	160		192	4
9[2]	36	q3 wks	40	80	160		360	4
10[1,2]	64	q3 wks	40	96	192	272	176	6

TNS, total neuropathy score; Ix, ixabepilone; Cy, cycle.
[1]History of smoking.
[2]Biopsies examined for Electron microscopic studies.

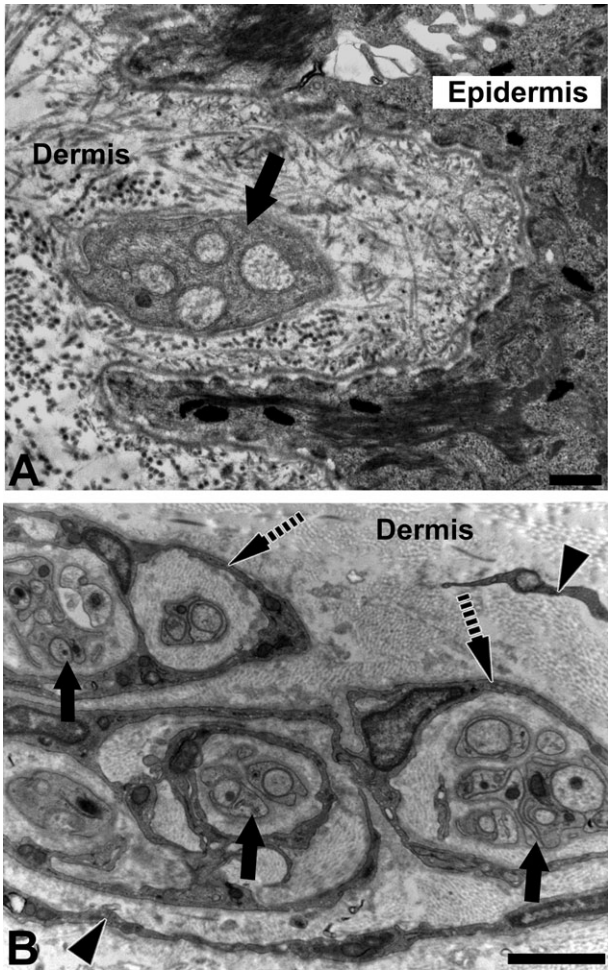

Figure 1. Subepidermal Remak Schwann cell and a small cutaneous nerve in distal leg. (A) Two Remak Schwann cells with unmyelinated axons (arrows) remaining in the papillary dermis. These have also been referred to as: subepidermal nerve bundles.[23] (B) A small cutaneous nerve in the deeper dermis containing many Remak Schwann cells with unmyelinated axons arranged in bundles (arrows) enclosed by perineurium (slashed arrow) and partly by epineurium (arrow head). Scale bars A and B = 2 μm.

pattern, individual Remak Schwann cell in the subepidermis and Remak Schwann cell bundles in small distal cutaneous nerves were identified using previously specified criteria (Fig. 1).[23,24] Digital photographs for morphometry were captured at a magnification of 8000–16,000× and the photos were uploaded onto an imaging platform of transmission electron microscope (iTEM) (Olympus, Münster, Germany). The figures were enlarged by 50%, and an individual linear array was used to measure the axonal diameter (cross-sectional area) and the number of unmyelinated axons per Remak Schwann cell was enumerated according to the established methodology.[24] Also, the number of mitochondria per axon was counted and the morphology was graded based on specified criteria, modified from previous studies: distortion of cristae, electron translucency, and shape irregularity (Table 2).[25,26] All analyses were performed blinded to the clinical data and control/Ix status.

Table 2. Ultrastructural grading of mitochondria in unmyelinated axons of Remak Schwann cells.

Grade 0	Normal architecture
Grade 1	Distortion of cristae
Grade 2	Loss of cristae and the matrix is homogenous
Grade 3	Matrix is electron dense and pyknotic with distortion of outer membranes
Grade 4	Electron dense, vacuolation, pleomorphic, and fragmentation

Statistics

All data are expressed as the mean ± SEM. Changes in axon diameter were assessed by Student's *t*-test. The distribution of number of axons per Remak Schwann cell was assessed by chi-square test. Changes in TNS and mitochondrial morphology with cumulative ixabepilone exposure were assessed through a mixed effects model accounting for longitudinal measurements within individuals. All analyses were performed using Stata 11.0 (Stata Corp., College Station, TX). TNSc results were correlated with various axonal parameters using Spearman correlation coefficient.

Results

Study subject demographics

For Ix-treated patients, the median age at study entry was 56.5 years (range 36–70 years) and the median stage at diagnosis was 2. All patients received prior MTSA-based therapy prior to entry onto this study. Five patients (50%) received adjuvant taxane, and all received at least one taxane in the metastatic setting. The median number of chemotherapy regimens received in the metastatic setting prior to study entry was 4 with a range of 1–8 prior chemotherapy regimens. Healthy control subjects had no signs or symptoms of peripheral neuropathy. They had no history of potential causes of peripheral neuropathy such as diabetes, vitamin deficiencies, alcohol use, or toxic exposures including chemotherapy. They had a median age of 56.6 years (range 38–66 years).

Neurological assessment

Increasing TNSc values were strongly associated with cumulative Ix exposure (Fig. 2). There was no difference between weekly or q3-week dose schedules (not shown). At baseline, Ix-treated subjects had higher TNSc values

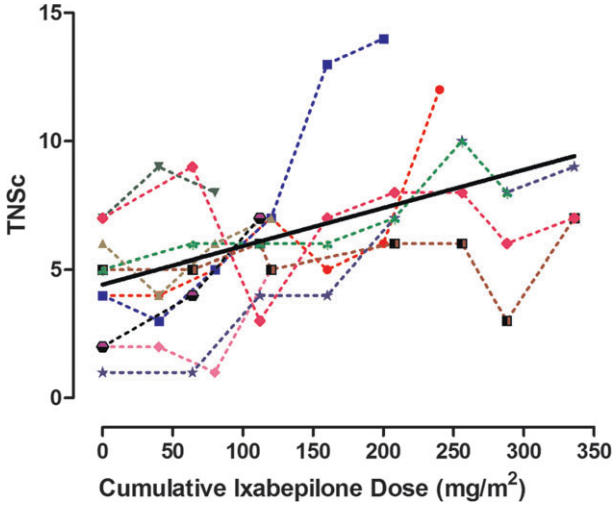

Figure 2. Peripheral neuropathy in ixabepilone-treated subjects. The total neuropathy score clinical progressively increased ($P \leq 0.0001$) with the total cumulative dose of Ixabepilone.

(4.5 ± 0.8 vs. controls: 0.0 ± 0.0) and with increasing cumulative Ix exposure we observed an increase in TNSc values (5.4 ± 1.2 at Cy3 and 10 ± 4 at Cy7 ($P < 0.0001$). Baseline TNSc and age were not associated with neuropathy progression.

Morphometry

A total of 226 axon profiles from controls and 442 profiles from Ix-treated patients were analyzed. In control subjects, Remak Schwann cells were arranged regularly and predominantly had 1–2 axons (53%) and 10% remained without axons. In Ix-treated subjects, there was an increase in denervated Remak Schwann cells from 29% at baseline to 39% by cycle 7 (mean cumulative dose of 250 mg/m^2) (Fig. 3A–C). Overall, there was a clear shift to the left in axon/Remak Schwann cell distribution ($P < 0.001$) with more denervated Schwann cells and fewer axons/Remak Schwann cell with increasing Ix exposure (Fig. 3B and C). The ratio of axons/Remak Schwann cell was strongly correlated with increasing chemotherapy cycles and cumulative dose ($R^2 = 0.98$, $P = 0.02$, Fig. 3C). With increasing TNSc scores, the number of axons per Remak Schwann cells showed a significant negative correlation (Spearman $r = -0.97$, $P = 0.004$). Taken together, these results are consistent with severe progressive axonal loss (Fig. 2) and corroborate the clinical data.

Axonal diameter

Axons were mildly dilated at baseline among patients who went on to receive Ix compared to control subjects (in nm, control: 354.9 ± 14.8; Ix-baseline: 422.9 ± 17; $P < 0.01$). These data are consistent with the Ix subjects having a mild baseline length-dependent neuropathy and is consistent with modestly elevated baseline TNS values. Axonal diameter significantly increased from baseline with increasing chemotherapy cycles (in nm, Cy3: 506.3 ± 22.1, Cy5: 534.8 ± 33, Cy7: 527.8 ± 24.4; $P < 0.001$) (Fig. 4A and B). On EM analysis, axons exhibited varying cytological features of degeneration: axons in varying sizes showing fragmentation of microtubules and neurofilaments resulting in granular debris, watery axoplasm, absence of axonal content, and accumulation of distended microvesicles and organelles of the lysosomal system (Fig. 4A and D). These findings are consistent with ixabepilone's described mechanism of action on microtubules. Distended axons ensheathed by retracted Schwann cell processes exposing the axons to the surrounding endoneurial collagen were noted, further hasten the degenerative processes (Fig. 4A), although many denervated Remak Schwann cells exhibited intact long mesaxons suggesting the preservation of a pathway for regeneration (Fig. 4C). In addition, cytological features of autophagy were seen, with axoplasm exhibiting compartmentalization and sequestration of neurofilaments clustering in the central portion of the axoplasm with lysosomal vesicles impinging on these degrading cytoplasmic contents (Fig. 4D).

Mitochondrial morphometry

Increasing ixabepilone cumulative exposure was associated with an increasing percentage of axon profiles with no mitochondria ($R^2 = 0.97$, Fig. 5A) and TNSc significantly correlated with the loss of mitochondria (Spearman $r = 0.97$, $P = 0.004$). This finding prompted us to examine mitochondria morphology using a grading system based on specific morphological criteria (Table 2).[27] In control subjects, 82% of axons had grade 0 (normal) or grade 1 morphology, whereas <4% had grade 4 morphology (Fig. 5B and C). Increasing ixabepilone exposure was strongly associated with an increase in the percentage of mitochondria with abnormal morphology (grades 3 and 4: baseline: 24%, Cy7: 79%, $P < 0.0001$, $R^2 = 0.94$, Figs. 5 and 6) and a corresponding decrease in the percentage with normal morphology (grades 0–1: baseline: 52%, Cy7: 2%, $P < 0.0001$, $R^2 = 0.97$, Fig. 5B) and showed a significant linear relationship with the clinical TNS scores (grades 3 and 4: $r = 0.97$, $P = 0.004$, grade 1–2: $r = -0.97$, $P = 0.004$). The axonal degeneration and mitochondrial changes were extensive and were observed both in subepidermal Remak Schwann cells and in small distal cutaneous nerves (Fig. 6B). Taken together, the dose-dependent depletion of mitochondria and the

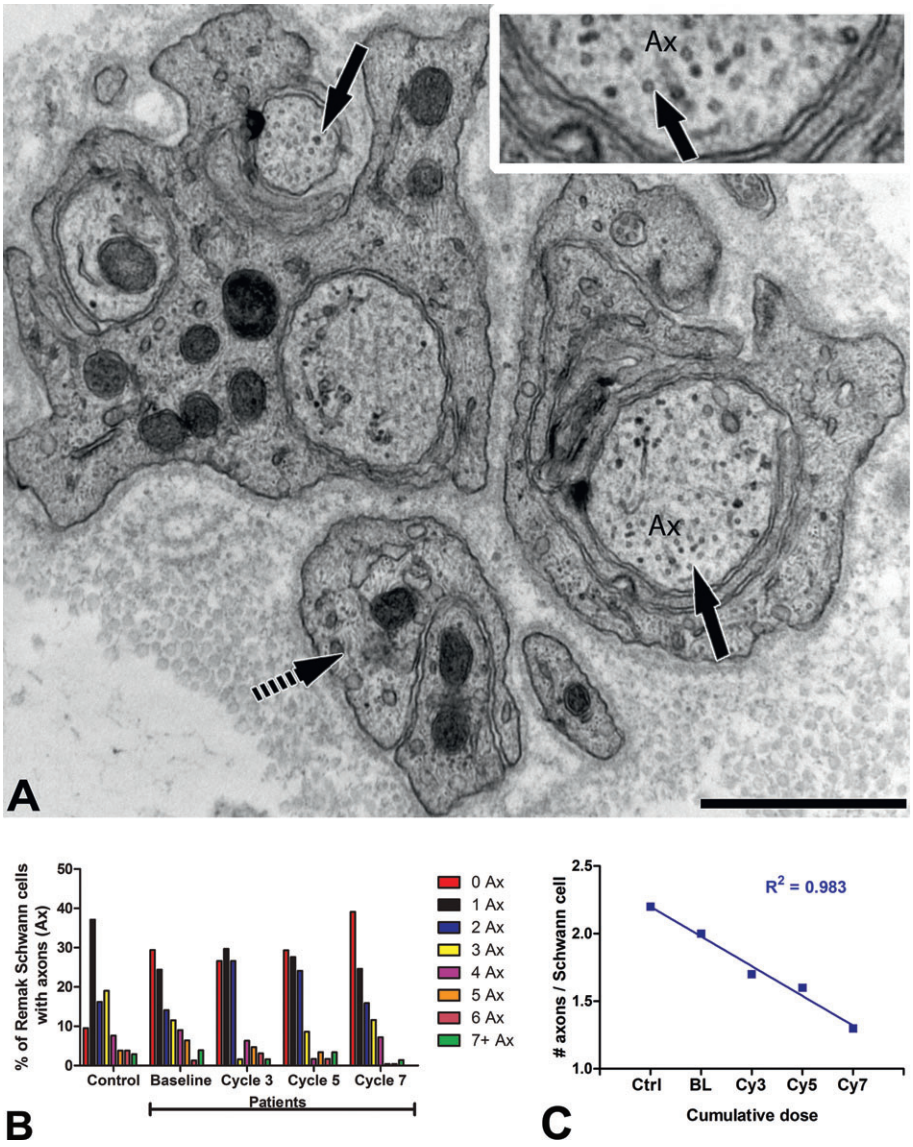

Figure 3. Remak Schwann cells in ixabepilone (Ix)-treated patients. (A) Electron micrograph of Remak Schwann cells containing normal axons with predominantly circular profiles (arrows, Ax-boxed) and few oblique profiles of microtubules. A slashed arrow identifies a denervated Remak Schwann cell. Scale bar = 1 μm. (B) The number of axons per Remak Schwann cells across the treatment group significantly decreased with increasing cumulative Ix dose, and was consistent with severe progressive axonal loss. In Ix-treated subjects, there was an increase in denervated Remak Schwann cells from 29% at baseline to 39% by cycle 7. The chi-square distribution for the different chemotherapy groups and the control group is highly significant ($P < 0.001$). (C) The number of axons per Schwann cell was linear and decreased with increasing cycle number ($P = 0.02$).

corresponding dose-dependent increase in abnormal morphology implicate a mechanism of mitochondrial toxicity. The observation of atypical large mitochondria of axons undergoing fragmentation suggests the possibility of ixabepilone affecting the fusion/fission dynamics of mitochondria and further studies are needed to confirm these findings.

Changes in other structures were also noted although they were less prominent. Occasional deep dermal myelinated axons identified showed degenerative changes with engulfment by macrophages. Perineuronal dermis surrounding degenerating Remak Schwann cells was cellular with stacks of lamellated Schwann cell processes (Fig. 6C), empty basal lamina, macrophages, and fibroblastic proliferation. Additionally, abnormal mitochondrial morphologies were observed in Remak Schwann cells and underscore the impact of Ix toxicity on supporting cells of axons with continuation of therapy. This sug-

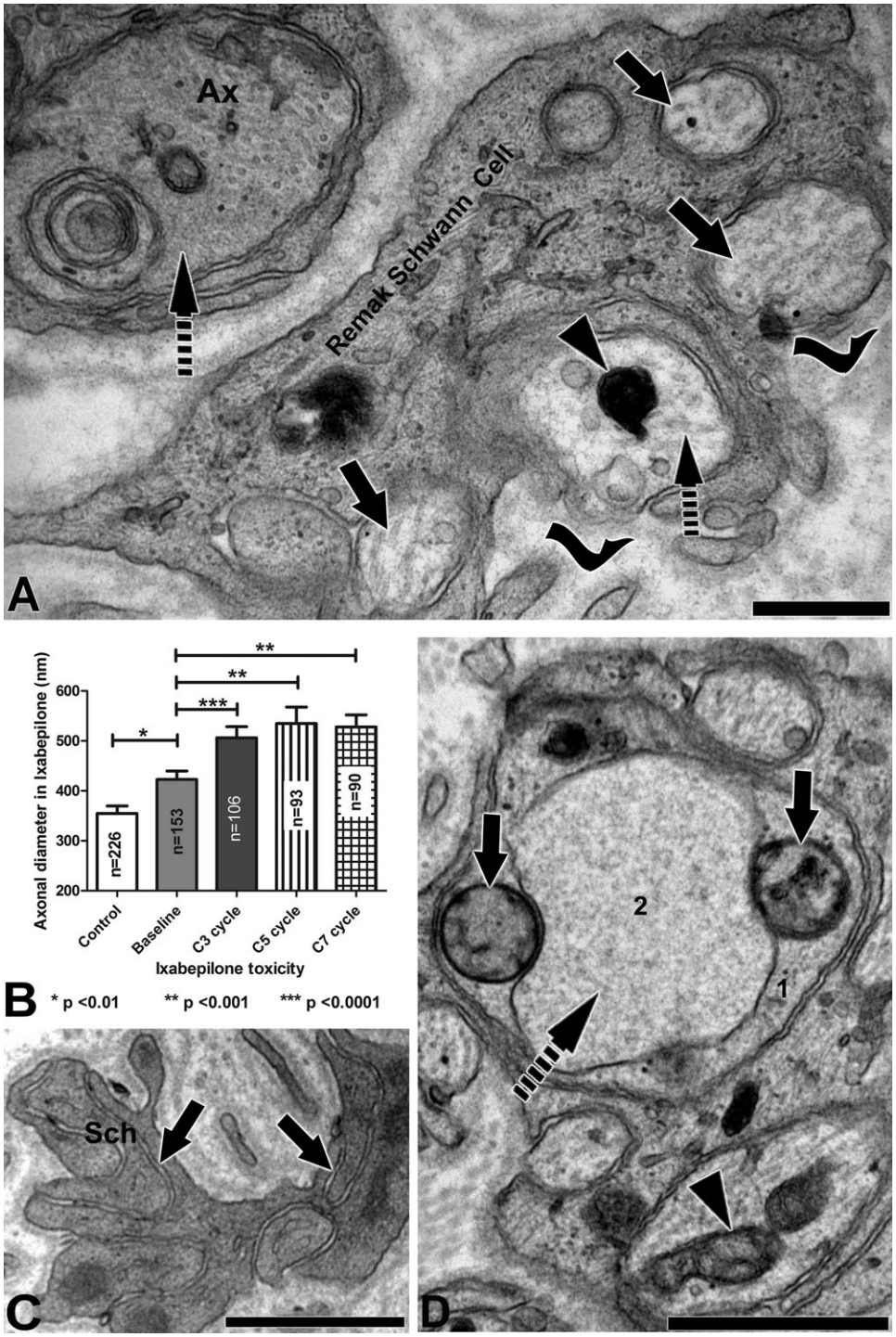

Figure 4. Electron micrographs of axonal changes in Ixabepilone-treated patients. (A) A distended axon (Ax) with part of the axoplasm (slashed arrow) undergoing degeneration. A large Remak Schwann cell containing degenerating axons in varying sizes (arrows), an axon exhibiting watery axoplasm with microvesicles (slashed arrow), and an atypical mitochondrion (arrow head). Portions of degenerating axonal membranes (warped arrows) are exposed to dermal collagen. (B) The axonal diameter in Ix-treated patients are larger and significantly increased from baseline. (C) A large Remak Schwann cell (Sch) with absence of axons but with preserved mesaxons (arrows). (D) A Remak Schwann cell with an axon (1) showing partitioned axoplasm with central sequestration (2) of degrading cytoskeletal structures (slashed arrow) and impinged by dilated lysosomal vesicles (arrows). The adjacent obliquely transected axon showing a long atypical mitochondria undergoing fragmentation (arrow head). Scale bars: A = 500 nm, C and D = 1 μm.

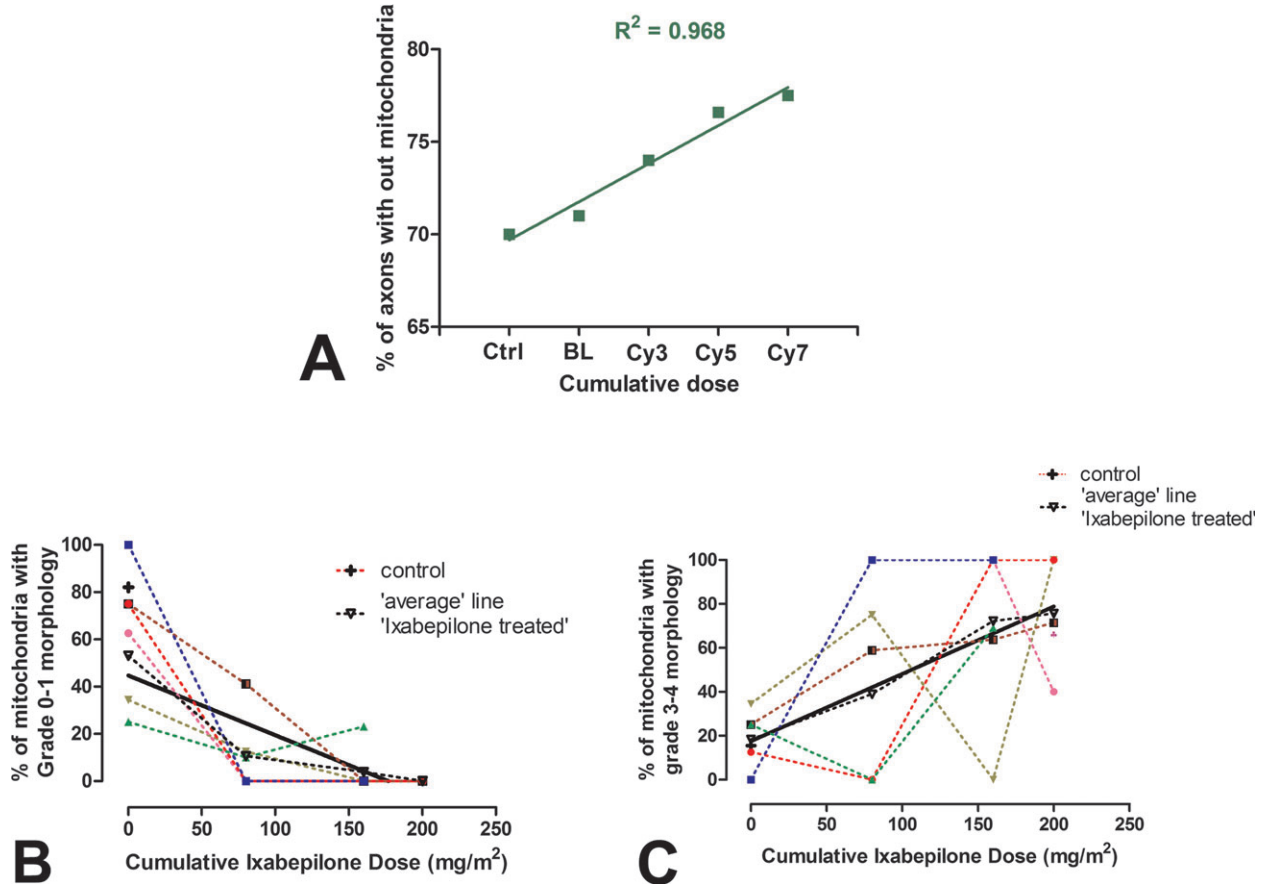

Figure 5. Effect of Ixabepilone on axonal mitochondria of Remak Schwann cells. (A) In patients with increasing chemotherapy cycles, axons trended toward progressive loss of mitochondria. (B) 82% of mitochondria from control subjects (baseline only) had normal (grade 0 or 1) morphology. Among Ix-treated subjects, there was a dose-dependent decrease in the percentage of mitochondria with normal (grade 0 or 1) morphology ($P < 0.001$). The thick black line represents the regression line for Ix-treated subjects. (C) After seven cycles of Ix (>200 mg/m^2), 79% of mitochondria exhibited severe atypical morphology (grade 3 or 4) compared to 15.5% of mitochondria from control subjects. Increasing cumulative ixabepilone exposure was strongly associated with an increase in the percentage of mitochondria with dysmorphic morphology ($P < 0.001$). The thick black line represents the regression line for Ix-treated subjects.

gests that loss of Schwann cell support may contribute to the ixabepilone-induced axonal degeneration that we observed.

Discussion

Chemotherapy-induced peripheral neuropathy is a significant cause of morbidity for cancer patients, the majority of which are potentially cured by their treatments. In order to implement improved strategies for identification of those at risk of PN and to formulate treatment strategies, one needs to understand the underlying biology at the neuronal level.

We examined the cutaneous nerves at the distal leg to understand the pathological mechanisms in ixabepilone-induced peripheral neuropathy. By ultrastructural analysis of 3-mm skin punches at baseline and at the third, fifth, and seventh cycle, we observed a distinct pattern of progressive cytopathological changes in unmyelinated axons of Remak Schwann cells and mitochondria.

First, we show that with increasing cumulative exposure, Remak Schwann cell-ensheathed axons undergo progressive degeneration, and after seven cycles nearly 45% of Remak Schwann cells are denervated. This axonal loss was paralleled by a corresponding increase in TNSc values. Second, we observed changes in the cross-sectional axonal diameter that significantly increased from the baseline diameter suggesting the action of ixabepilone on axonal caliber that is maintained by βIII tubulins and neurofilaments. Thirdly, there was active clearance of axonal debris by autophagosomes in Remak Schwann cells as well as by dermal macrophages and the preserved mesaxons indicate cytological features favoring a pathway for regeneration. Finally, we provide morphological evidence

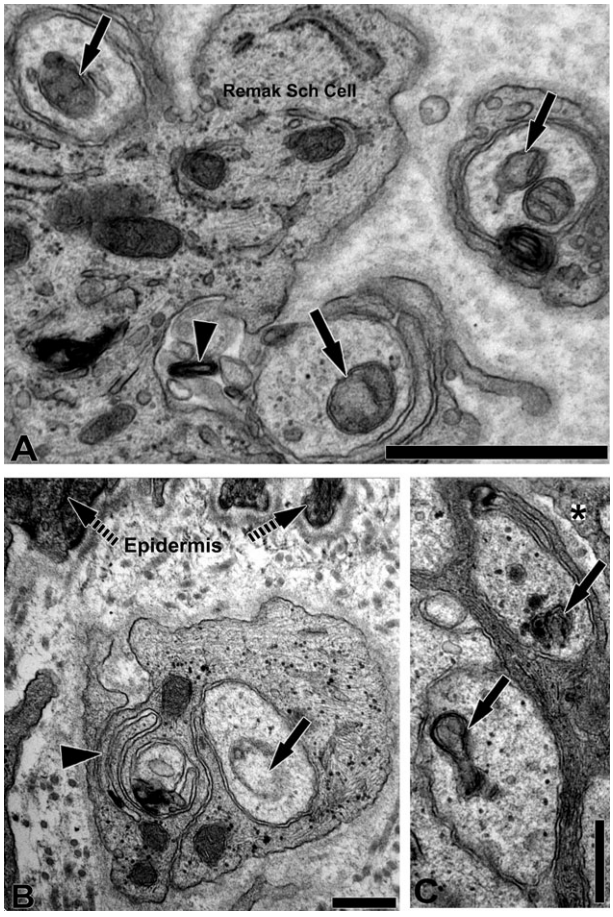

Figure 6. Electron micrographs of axonal mitochondrial changes of Remak Schwann cells in Ixabepilone-treated patients. (A) Axons of Remak Schwann cell exhibiting atypical mitochondria with loss of cristae and homogenous matrix (arrows). An autophagosome (arrow head) is seen adjacent to a degenerating axon with atypical mitochondria. (B) A subepidermal (epidermis-slashed arrows) Remak Schwann cell with the axonal mitochondria showing vacuolization (arrow), and stacking of lamellated Schwann cell processes (arrow head). (C) A small cutaneous nerve bundle (* perineurium) with the axons exhibiting atypical mitochondria undergoing fragmentation (arrows). Scale bars: A = 1 μm, B and C = 500 nm.

that Ix targets mitochondria with a dose-dependent reduction in mitochondria and a dose-dependent increase in abnormal mitochondrial morphology.

Ix-induced neuropathy is accompanied by unmyelinated axonal loss

Both taxanes and epothilones exert antineoplastic effects through microtubule stabilization which impairs cell cycle progression.[28,29] The effect of taxane on peripheral nerves has been extensively investigated; however, the primary target of taxane on peripheral nerves is still debatable. Disruption of protein and axonal flow in the nerves is considered generally as a possible mechanism for taxane-induced neuropathy.[30,31] It has been shown that a cumulative intraperitoneal dose of 8–80 mg/kg paclitaxel produces various degrees of degeneration in the sciatic nerve, peroneal nerve, and dorsal roots[32] and decrease in intraepidermal nerve fiber density with intravenous dose.[33] But low intraperitoneal doses of 2–18 mg/kg paclitaxel did not cause degeneration in sciatic and sural nerves suggesting differential effect of drug on peripheral nerves.[21,34] In our study, Ix administration induced degenerative changes with axonal loss in a dose-dependent fashion that involved the distal unmyelinated axons of Remak Schwann cells. This pattern of cumulative toxicity with Ix follows the pattern defined in rodent models of Taxol-induced peripheral neuropathy.[35]

Ix on cytoskeletal structures of unmyelinated axons

One would anticipate that binding and stabilization of cellular microtubules by epothilone B and taxanes would result in increased microtubule density and clustering. In fact, we observed that cumulative Ix exposure altered the cytoskeletal architecture and significantly increased the axonal diameter from baseline to swollen at cumulative doses of 80–90 mg/m^2. This is consistent with the known effects of βIII tubulins and neurofilaments on axonal caliber.[36,37] While axonal caliber increased, the cytoskeletal architecture was abnormal and was associated with axonal loss suggesting that Ix had effects beyond those on cytoskeletal elements.

Toxicity to unmyelinated axonal mitochondria

A striking finding of this study was the progressive loss of mitochondria in unmyelinated axons of Remak Schwann cells combined with a dose-dependent mitochondrial morphological derangement. It is generally presumed that new mitochondria are generated in the cell body, transported down to distal locations, and appropriate distribution of functional mitochondria at the distal axons are maintained by fusion and fission dynamics.[38] Furthermore, neuronal mitochondria provide energy by generating adenosine triphosphate (ATP) that is required for axonal transport.[36,39,40] Microtubules play a critical role in axonal flow in peripheral nerves. Axonal transport disruption has been reported in β,β-iminodipropionitrile (IDPN), acrylamide as well as in taxoid-induced toxic neuropathies.[41,42] Most peripheral neuropathies including HIV-SN, diabetic, and toxic neuropathies present as a length-dependent, "dying back" axonopathy, in which

axonal degeneration starts in the distal terminals and continues in a centripetal direction. The long unmyelinated axons of distal limbs that project to the skin have a high density of mitochondria relative to their large myelinated counterparts and studies have demonstrated the accumulation of abnormal mitochondria in distal unmyelinated axons and higher mtDNA deletion mutations in distal nerve segments in patients affected by HIV-SN.[24,43,44] In painful peripheral neuropathy induced by 2′3′-dideoxycytidine (ddC) and paclitaxel[21,45] swollen and vacuolated mitochondria have been reported.

In our study, 79% of axonal mitochondria from subjects with cumulative exposures above 200 mg/m^2 showed abnormal morphology that ranged from complete effacement of cristae to abnormally large mitochondria with vacuolation and fragmentation of mitochondria. Similarly, although less pronounced, changes were observed in the mitochondria of ensheathing Remak Schwann cells, suggesting that disruption of Remak Schwann cell support may also contribute to axon loss. Tubulin is an integral protein of the mitochondrial membranes, and plays a role in the transport of mitochondria along microtubules.[46,47] Therefore, we postulate that Ix binds to the mitochondrial membranes inducing a dose-dependent mitochondrial injury, fragmentation and death, which, in turn, induces axonal necrosis secondary to energy failure.

We observed active lysosomal vesicles and autophagosomal changes in degenerating axons as well as macrophages in proximity to Remak Schwann cells. This appearance is typical of macrophage activation and recruitment to the site of nerve injury. These macrophages may remove axonal debris, induce Remak Schwann cell proliferation, and stimulate nerve growth factor release which sets the stage for future nerve regeneration.[48–50] The presence of macrophages combined with the preserved mesaxons in Remak Schwann cells suggests that there is active clearance of axonal debris providing a foundation for axonal recovery and regeneration. These pathological features support the clinical impression that ixabepilone-induced CIPN has a reversible component and toxicity can be mitigated through dose reduction and delays.[51]

Conclusion

Our study demonstrates complimentary ultrastructural and clinical evidence that ixabepilone induces dose-dependent toxicity to distal unmyelinated nerve fibers. Toxicity was observed in the form of mitochondrial loss, disruption of normal mitochondrial structure, disintegration of axonal content, and progressive axon loss. As similar, although less pronounced, changes were seen among Schwann cell mitochondria, these observations suggest mitochondrial dysfunction and oxidative stress as a mechanism of toxicity. Serial skin biopsy-based analyses are well suited to monitor the neurotoxicity of chemotherapeutic agents.

Acknowledgments

We thank all patients involved in this study. The authors thank Carol Cooke and Peter Hauer for their expert technical assistance. This work was presented at the Peripheral Nerve Society meeting, June 29-July 3, 2013, St. Malo, Brittany, France. Bristol Myers Squibb Oncology (BMSO) and the Anne Moore Breast Cancer Research Fund provided partial funding for this study. BMSO also provided study drug.

Authors Contribution

L. T. V. designed the study, coordinated acquisition of clinical data, followed the study participants, and provided scientific and operational advice during the study. K. C. followed the study participants, and oversaw acquisition of patient samples. D. D., M. C., A. M., T. C., E. C., followed the study participants, M. W., M. L., and A. R. oversaw the acquisition of patient samples, M. P. coordinated the laboratory analyses, statistical analysis and data interpretation. G. J. E performed electron micrograph interpretation and analysis, G. J. E., K. C., M. P., and L. T. V. critically reviewed clinical and laboratory data. All authors approved the final version of the manuscript.

Conflict of Interest

None declared.

References

1. Jemal A, Murray T, Ward E, et al. Cancer statistics, 2005. CA Cancer J Clin 2005;55:10–30.
2. Howlader N, Noone AM, Yu M, et al. Use of imputed population-based cancer registry data as a method of accounting for missing information: application to estrogen receptor status for breast cancer. Am J Epidemiol 2012;176:347–356.
3. Schiff PB, Fant J, Horwitz SB. Promotion of microtubule assembly in vitro by taxol. Nature 1979;277:665–667.
4. Vahdat LT, Papadopoulos K, Balmaceda C, et al. Phase I trial of sequential high-dose chemotherapy with escalating dose paclitaxel, melphalan, and cyclophosphamide, thiotepa, and carboplatin with peripheral blood progenitor support in women with responding metastatic breast cancer. Clin Cancer Res 1998;4:1689–1695.
5. Perez EA, Lerzo G, Pivot X, et al. Efficacy and safety of ixabepilone (BMS-247550) in a phase II study of patients

with advanced breast cancer resistant to an anthracycline, a taxane, and capecitabine. J Clin Oncol 2007;25:3407–3414.
6. Roche H, Yelle L, Cognetti F, et al. Phase II clinical trial of ixabepilone (BMS-247550), an epothilone B analog, as first-line therapy in patients with metastatic breast cancer previously treated with anthracycline chemotherapy. J Clin Oncol 2007;25:3415–3420.
7. Thomas E, Tabernero J, Fornier M, et al. Phase II clinical trial of ixabepilone (BMS-247550), an epothilone B analog, in patients with taxane-resistant metastatic breast cancer. J Clin Oncol 2007;25:3399–3406.
8. Chaudhry V, Rowinsky EK, Sartorius SE, et al. Peripheral neuropathy from taxol and cisplatin combination chemotherapy: clinical and electrophysiological studies. Ann Neurol 1994;35:304–311.
9. Nurgalieva Z, Xia R, Liu CC, et al. Risk of chemotherapy-induced peripheral neuropathy in large population-based cohorts of elderly patients with breast, ovarian, and lung cancer. Am J Ther 2010;17:148–158.
10. Sparano JA, Vrdoljak E, Rixe O, et al. Randomized phase III trial of ixabepilone plus capecitabine versus capecitabine in patients with metastatic breast cancer previously treated with an anthracycline and a taxane. J Clin Oncol 2010;28:3256–3263.
11. Bunnell C, Vahdat L, Schwartzberg L, et al. Phase I/II study of ixabepilone plus capecitabine in anthracycline-pretreated/resistant and taxane-resistant metastatic breast cancer. Clin Breast Cancer 2008;8: 234–241.
12. Denduluri N, Low JA, Lee JJ, et al. Phase II trial of ixabepilone, an epothilone B analog, in patients with metastatic breast cancer previously untreated with taxanes. J Clin Oncol 2007;25:3421–3427.
13. Vahdat LT, Thomas ES, Roche HH, et al. Ixabepilone-associated peripheral neuropathy: data from across the phase II and III clinical trials. Support Care Cancer 2012;20:2661–2668.
14. Chiorazzi A, Nicolini G, Canta A, et al. Experimental epothilone B neurotoxicity: results of in vitro and in vivo studies. Neurobiol Dis 2009;35:270–277.
15. Bollag DM, McQueney PA, Zhu J, et al. Epothilones, a new class of microtubule-stabilizing agents with a taxol-like mechanism of action. Cancer Res 1995;55:2325–2333.
16. Altmann KH, Wartmann M, O'Reilly T. Epothilones and related structures – a new class of microtubule inhibitors with potent in vivo antitumor activity. Biochim Biophys Acta 2000;1470:M79–M91.
17. Morris PG, Fornier MN. Microtubule active agents: beyond the taxane frontier. Clin Cancer Res 2008;14:7167–7172.
18. Giannakakou P, Gussio R, Nogales E, et al. A common pharmacophore for epothilone and taxanes: molecular basis for drug resistance conferred by tubulin mutations in human cancer cells. Proc Natl Acad Sci USA 2000;97:2904–2909.
19. Polydefkis M, Hauer P, Griffin JW, et al. Skin biopsy as a tool to assess distal small fiber innervation in diabetic neuropathy. Diabetes Technol Ther 2001;3:23–28.
20. Gibbons CH, Griffin JW, Polydefkis M, et al. The utility of skin biopsy for prediction of progression in suspected small fiber neuropathy. Neurology 2006;66:256–258.
21. Flatters SJ, Bennett GJ. Studies of peripheral sensory nerves in paclitaxel-induced painful peripheral neuropathy: evidence for mitochondrial dysfunction. Pain 2006;122:245–257.
22. Cavaletti G, Jann S, Pace A, et al. Multi-center assessment of the total neuropathy score for chemotherapy-induced peripheral neurotoxicity. J Peripher Nerv Syst 2006;11:135–141.
23. Bennett GJ, Liu GK, Xiao WH, et al. Terminal arbor degeneration – a novel lesion produced by the antineoplastic agent paclitaxel. Eur J Neurosci 2011;33:1667–1676.
24. Ebenezer GJ, McArthur JC, Thomas D, et al. Denervation of skin in neuropathies: the sequence of axonal and Schwann cell changes in skin biopsies. Brain 2007;130:2703–2714.
25. Kong J, Xu Z. Massive mitochondrial degeneration in motor neurons triggers the onset of amyotrophic lateral sclerosis in mice expressing a mutant SOD1. J Neurosci 1998;18:3241–3250.
26. Solenski NJ, diPierro CG, Trimmer PA, et al. Ultrastructural changes of neuronal mitochondria after transient and permanent cerebral ischemia. Stroke 2002;33:816–824.
27. Daugherty CC, Gartside PS, Heubi JE, et al. A morphometric study of Reye's syndrome. Correlation of reduced mitochondrial numbers and increased mitochondrial size with clinical manifestations. Am J Pathol 1987;129:313–326.
28. Jordan MA, Wilson L. Microtubules as a target for anticancer drugs. Nat Rev Cancer 2004;4:253–265.
29. Jordan MA, Wendell K, Gardiner S, et al. Mitotic block induced in HeLa cells by low concentrations of paclitaxel (Taxol) results in abnormal mitotic exit and apoptotic cell death. Cancer Res 1996;56:816–825.
30. Argyriou AA, Koltzenburg M, Polychronopoulos P, et al. Peripheral nerve damage associated with administration of taxanes in patients with cancer. Crit Rev Oncol Hematol 2008;66:218–228.
31. Carlson K, Ocean AJ. Peripheral neuropathy with microtubule-targeting agents: occurrence and management approach. Clin Breast Cancer 2011;11:73–81.
32. Cavaletti G, Cavalletti E, Oggioni N, et al. Distribution of paclitaxel within the nervous system of the rat after repeated intravenous administration. Neurotoxicology 2000;21:389–393.

33. Lauria G, Lombardi R, Borgna M, et al. Intraepidermal nerve fiber density in rat foot pad: neuropathologic-neurophysiologic correlation. J Peripher Nerv Syst 2005;10:202–208.
34. Polomano RC, Mannes AJ, Clark US, et al. A painful peripheral neuropathy in the rat produced by the chemotherapeutic drug, paclitaxel. Pain 2001;94:293–304.
35. Cavaletti G, Cavalletti E, Montaguti P, et al. Effect on the peripheral nervous system of the short-term intravenous administration of paclitaxel in the rat. Neurotoxicology 1997;18:137–145.
36. Friede RL, Samorajski T. Axon caliber related to neurofilaments and microtubules in sciatic nerve fibers of rats and mice. Anat Rec 1970;167:379–387.
37. Persohn E, Canta A, Schoepfer S, et al. Morphological and morphometric analysis of paclitaxel and docetaxel-induced peripheral neuropathy in rats. Eur J Cancer 2005;41:1460–1466.
38. Haun F, Nakamura T, Lipton SA. Dysfunctional mitochondrial dynamics in the pathophysiology of neurodegenerative diseases. J Cell Death 2013;6:27–35.
39. Friede RL, Ho KC. The relation of axonal transport of mitochondria with microtubules and other axoplasmic organelles. J Physiol 1977;265:507–519.
40. Blaker WD, Goodrum JF, Morell P. Axonal transport of the mitochondria-specific lipid, diphosphatidylglycerol, in the rat visual system. J Cell Biol 1981;89:579–584.
41. Griffin JW, Fahnestock KE, Price DL, et al. Microtubule-neurofilament segregation produced by beta, beta'-iminodipropionitrile: evidence for the association of fast axonal transport with microtubules. J Neurosci 1983;3:557–566.
42. Gold BG, Griffin JW, Price DL. Slow axonal transport in acrylamide neuropathy: different abnormalities produced by single-dose and continuous administration. J Neurosci 1985;5:1755–1768.
43. Lehmann HC, Chen W, Borzan J, et al. Mitochondrial dysfunction in distal axons contributes to human immunodeficiency virus sensory neuropathy. Ann Neurol 2010;69:100–110.
44. Bristow EA, Griffiths PG, Andrews RM, et al. The distribution of mitochondrial activity in relation to optic nerve structure. Arch Ophthalmol 2002;120:791–796.
45. Dalakas MC, Semino-Mora C, Leon-Monzon M. Mitochondrial alterations with mitochondrial DNA depletion in the nerves of AIDS patients with peripheral neuropathy induced by 2′3′-dideoxycytidine (ddC). Lab Invest 2001;81:1537–1544.
46. Carre M, Andre N, Carles G, et al. Tubulin is an inherent component of mitochondrial membranes that interacts with the voltage-dependent anion channel. J Biol Chem 2002;277:33664–33669.
47. Ball EH, Singer SJ. Mitochondria are associated with microtubules and not with intermediate filaments in cultured fibroblasts. Proc Natl Acad Sci USA 1982;79:123–126.
48. Lu X, Richardson PM. Responses of macrophages in rat dorsal root ganglia following peripheral nerve injury. J Neurocytol 1993;22:334–341.
49. Perry VH, Brown MC. Macrophages and nerve regeneration. Curr Opin Neurobiol 1992;2:679–682.
50. Shin YK, Jang SY, Lee HK, et al. Pathological adaptive responses of Schwann cells to endoplasmic reticulum stress in bortezomib-induced peripheral neuropathy. Glia 2010;58:1961–1976.
51. Vahdat L. Ixabepilone: a novel antineoplastic agent with low susceptibility to multiple tumor resistance mechanisms. Oncologist 2008;13:214–221.

